Comparative reservoir competence of inbred *Peromyscus leucopus*, C57BL/6J, and C3H/HeN for *Borrelia burgdorferi* B31

Short Title: *Reservoir competence of Peromyscus leucopus and mice for B. burgdorferi B31*

Jeffrey S. Bourgeois[1,2], Stephanie S. You[1,2], Luke H. Clendenen[1,2], Muskan Shrestha[1,2], Tanja Petnicki-Ocwieja[1,2], Sam R Telford III[2,3], Linden T. Hu[1,2,#]

1. Tufts University, Department of Molecular Biology and Microbiology, Boston, MA, United States of America
2. Tufts University, Tufts Lyme Disease Initiative, Boston, MA, United States of America
3. Tufts University, Department of Infectious Disease and Global Health, Tufts University, North Grafton, MA, United States of America

Corresponding Author: linden.hu@tufts.edu

Abstract

The Lyme disease spirochete *Borrelia burgdorferi* causes a range of acute and chronic maladies in humans and other incidental hosts infected with the pathogen. However, a primary vertebrate reservoir, *Peromyscus leucopus*, is reported not to have reduced fitness following infection. One hypothesis for this observation is that *P. leucopus* and *B. burgdorferi* exist symbiotically: *P. leucopus* restrain their immune response against the microbe and enable the enzootic cycle while *B. burgdorferi* avoids causing damage to the host. While aspects of this hypothesis have been tested, the exact interactions that occur between *P. leucopus* and *B. burgdorferi* during infection remain understudied. Here we compared infection of *P. leucopus* with *B. burgdorferi* B31 with infection of the traditional *B. burgdorferi* murine models—C57BL/6J and C3H/HeN *Mus musculus*, which develop signs of inflammation akin to human disease. We find that *B. burgdorferi* were able to reach much higher burdens in *M. musculus*, and that the overall kinetics of infection differed between the two rodent species. We also found that *P. leucopus* remained infectious to larval *Ixodes scapularis* for a far shorter period than either *M. musculus* strain. In line with these observations, we found that *P. leucopus* does launch a modest but sustained inflammatory response against *B. burgdorferi* in the skin, which we hypothesize leads to reduced bacterial viability and infectivity in these hosts. Similarly, we also observe evidence of inflammation in infected *P. leucopus* hearts. These observations provide new insight into reservoir species and the *B. burgdorferi* enzootic cycle.

Author Summary

The bacteria that cause Lyme disease, *Borrelia burgdorferi*, must alternate between infecting a vertebrate host—usually rodents or birds—and ticks. In order to be successful in that endeavor the bacteria must avoid being killed by the vertebrate host before it can infect a new larval tick. In this work we examine how *B. burgdorferi* and one of its primary vertebrate reservoirs, *Peromyscus leucopus*, interact during an experimental infection. We find that *B. burgdorferi* appear to colonize its natural host less successfully than conventional laboratory mouse models which aligns with a sustained seemingly anti-bacterial response by *P. leucopus* against the microbe. These data question long-held assumptions about *P. leucopus* immunology and could potentially serve as a foundation to uncover ways to disrupt the spread of *B. burgdorferi* in nature.

Keywords

Peromyscus leucopus, Borrelia burgdorferi, Borreliella burgdorferi, Lyme disease, Ixodes scapularis, vector-borne disease, tick-borne disease, enzootic cycle

Introduction

Few endemic pathogens in the United States are as infamous as *Borrelia burgdorferi* sensu stricto (also called *Borreliella burgdorferi*), or the "Lyme disease spirochete," which causes a range of acute and chronic disease symptoms in humans. In North America, *B. burgdorferi* is spread between vertebrate hosts by the "deer tick" or "black-legged tick" *Ixodes scapularis* [1-3]. This enzootic cycle occurs ad infinitum as larval ticks acquire *B. burgdorferi* from infected vertebrates, molt, transmit the infection to new vertebrate hosts as nymphal ticks, molt into adult ticks, and produce new larval ticks [4]. While *B. burgdorferi* can infect numerous permissive vertebrate hosts ranging from birds [5] to dogs [6], one of the dominant North American reservoir host for *B. burgdorferi* is the white-footed mouse *Peromyscus leucopus* [7]. By some estimates, *P. leucopus* accounts for ~30% of *B. burgdorferi* spread into larval ticks [8], though the exact value likely varies by region and year. This aligns with other work which noted that in endemic regions, up to ~30-95% of this highly abundant rodent are infected with *B. burgdorferi* [9, 10]. Numerous ecological and laboratory studies have noted a unique relationship between *B. burgdorferi* and *P. leucopus* as, outside of neonate infection [11], *B. burgdorferi* has no detectable impact on *P. leucopus* fitness [10] and has not been reported to drive any observed behavioral [12, 13] or histological [11] changes. Even at the molecular level, two studies found very few changes to gene expression during post-acute infection (4-5 weeks post infection) in skin [14] or late infection (10 weeks post infection) in spleen [15]. The transcriptomic inflammatory response is limited despite considerable evidence that *P. leucopus* remain colonized by *B. burgdorferi* for months following infection [10, 16, 17].

One hypothesis that could explain these findings is that *P. leucopus* and the Lyme disease spirochete exist in a sort of truce throughout the infection: *P. leucopus* does not try to eradicate the pathogen following infection and in return *B. burgdorferi* does not cause any detectable damage. While this hypothesis is well-grounded in parasitism theory, as long co-existence between parasites and hosts is often thought to result in mutualism [18], the extent to which *B. burgdorferi* are allowed to freely replicate and survive in *P. leucopus* compared to other hosts has not been thoroughly tested. However, some data suggests that *P. leucopus* are not as effective at infecting ticks with *B. burgdorferi* compared with C3H laboratory mice [17], though it is unclear whether these results correlated with differences in bacterial fitness within the rodent hosts. Other work has also demonstrated that strains more closely associated with avian hosts have reduced fitness in *P. leucopus* [19]. These results appear to argue against a broad *P. leucopus-B. burgdorferi* mutualistic relationship.

Here we seek to examine the relationship between *P. leucopus* and *B. burgdorferi* by examining host and bacterial dynamics throughout infection. Using the *B. burgdorferi* B31 type-strain, we compare *B. burgdorferi* burden dynamics in inbred *P. leucopus* as well as two inbred *Mus musculus* mouse strains (C57BL/6J and C3H/HeN) and find that *P. leucopus* restrain *B. burgdorferi* burden compared to the laboratory mouse strains. This correlates with a modest transcriptional burst of genes associated with innate and adaptive immunity in the skin and very mild carditis in *P. leucopus*, suggesting that *P. leucopus* are actively responding to and controlling *B. burgdorferi* B31 infection. Notably, infected *P. leucopus* transmit less *B. burgdorferi* to *I. scapularis* larvae than similarly infected laboratory mouse strains. Together, these data demonstrate that despite being a core reservoir for *B. burgdorferi*, *P. leucopus* exerts a substantial immune pressure on at least some *B. burgdorferi* strains—including B31, during the enzootic cycle.

Results

Inbred *Peromyscus leucopus* restrict *Borrelia burgdorferi* B31 during early infection.

Substantial work has demonstrated that *P. leucopus* respond to the bacterial pathogen associated molecular pattern lipopolysaccharide (LPS) to a far lesser extent than inbred (BALB/c) [20] and outbred (CD-1) [21] *M. musculus.* While *B. burgdorferi* lacks LPS, if bacterial sensing is broadly suppressed in *P. leucopus*, *B. burgdorferi* could be allowed to thrive until the bacteria is collected during another tick bloodmeal. To test whether *P. leucopus* is more permissive to *B. burgdorferi* during early infection, we injected inbred *P. leucopus* and two inbred *M. musculus* strains (C57BL/6J and C3H/HeN) subcutaneously with $1x10^5$ *B. burgdorferi* B31 spirochetes and collected skin from the injection site one week later. Note that these *M. musculus* strains were chosen because they have routinely been used to model *B. burgdorferi* infectivity [22-27], and C3H have previously been used as a comparator when studying *Peromyscus-Borrelia* interactions [15, 17, 28]. Further, while *B. burgdorferi* B31 likely does not recapitulate all host-*B. burgdorferi* interactions that occur in nature, it is the *B. burgdorferi* type strain and has been thoroughly described in the past, and thus we chose to focus these studies on this strain.

We hypothesized that if *P. leucopus* are highly permissive to *B. burgdorferi*, the microbe would be able to reach higher bacterial burdens than in *M. musculus*. While we were able to culture spirochetes from the injection site of all the tested rodents **(Figure 1A)**, we found that *P. leucopus* had equal bacterial burdens (calculated by quantifying bacterial genomic DNA copies by digital droplet PCR [ddPCR]) at the injection site as C57BL/6J mice but substantially lower bacterial burden compared to C3H/HeN mice **(Figure 1B)**. This suggests that, contrary to our hypothesis, *P. leucopus* are less permissive to *B. burgdorferi* B31 than C3H/HeN mice.

While the *B. burgdorferi* subcutaneous injection model offers many advantages, it does not always accurately recapitulate wild infection where *I. scapularis* deliver a small number of *B. burgdorferi* and saliva proteins into the host during the bloodmeal. In order to better replicate natural infections, we infected rodents by placing five infected *I. scapularis* nymphs on the backs of *P. leucopus* and *M. musculus*. We then harvested skin from the tick placement site one week later. Again, we successfully cultured spirochetes out of all of the tick placement sites **(Figure 1C)**, but this time we found that *P. leucopus* had substantially (~100x) lower bacterial burdens at the placement site compared to either C57BL/6J or C3H/HeN mice **(Figure 1D)**. Thus, we conclude that despite being a primary vertebrate host for *B. burgdorferi* and *I. scapularis* in North America [7], our inbred *P. leucopus* are far less permissive to high *B. burgdorferi* B31 burdens immediately following tick bite.

To understand the long-term impacts of the reduced bacterial numbers in *P. leucopus* we tracked bacterial burdens in individual rodents infected by nymphal ticks over time, taking weekly ear punches over one month. We found that similar to our findings at the tick placement site *P. leucopus* had reduced bacterial burdens at early time points compared to the *M. musculus* strains **(Figure 1E)**. While both *M. musculus* strains had their peak infection at approximately 2.5 weeks post-nymph placement, we did not observe substantial increases in bacterial burdens in *P. leucopus* until 3.5-4.5 weeks post-nymph placement. This demonstrated not only that *P. leucopus* also appears to be less permissive to *B. burgdorferi* B31 in this secondary skin site, but that the overall infection kinetics in *P. leucopus* are substantially

different than in the model species as indicated by a significant interaction term in our Two-Way ANOVA ($p_{rodent\ x\ time}$= 0.05).

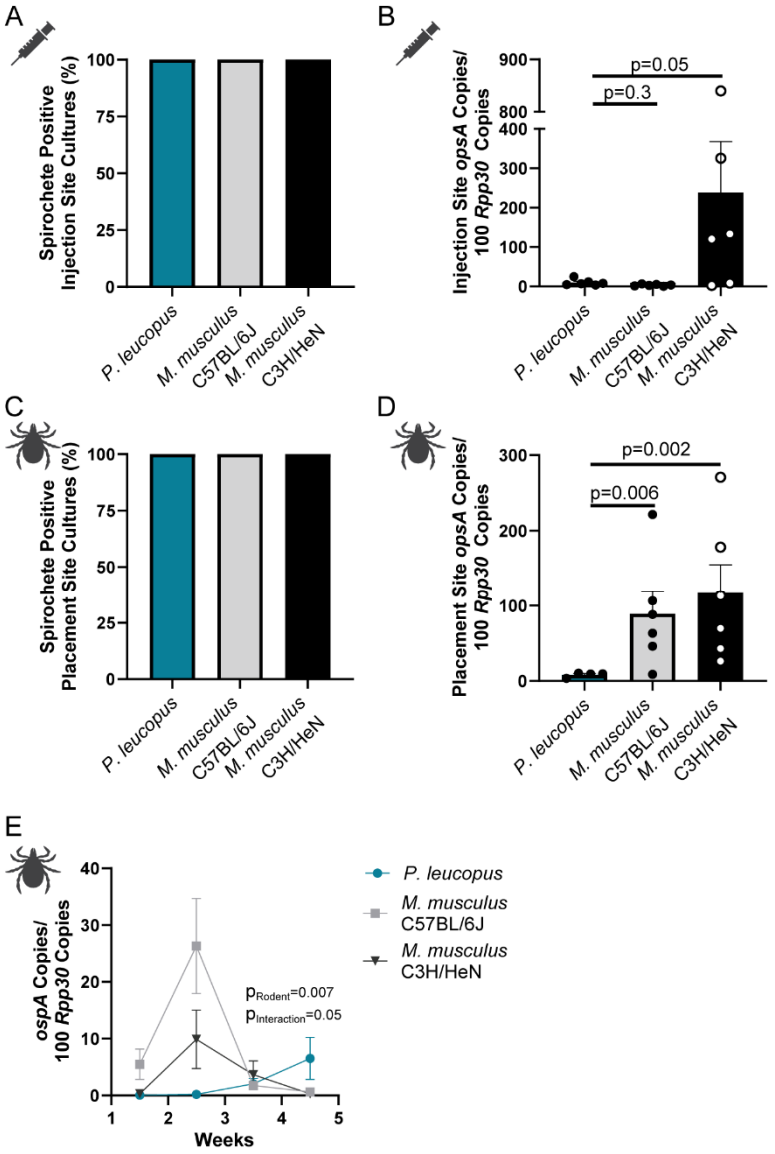

Figure 1: *B. burgdorferi* B31 expand to greater numbers in *M. musculus* than in *P. leucopus* following tick bite. (A) *B. burgdorferi* can be cultured from needle injection sites from *P. leucopus* and *M. musculus* (n=6) one week post injection. (B) *B. burgdorferi* are present at substantially lower numbers at the needle injection site in *P. leucopus* than C3H/HeN mice by ddPCR. For panels A and B rodents were injected with 100,000 *B. burgdorferi* in 200 µL of BSK-II via subcutaneous injection. (C) *B. burgdorferi* can be cultured from tick placement sites one week post infestation. (D) *B. burgdorferi* are present at substantially lower numbers at the tick placement site in *P. leucopus* (n=4) than C57BL/6J (n=6) or C3H/HeN (n=6) one week post infestation by ddPCR. For panels C and D, five infected nymphal *I. scapularis* were placed in a tick containment chamber on each rodent's back. The space under the containment chamber was harvested one week post infestation. For panels A and C, cultures were

monitored for spirochetes for three weeks. For Panels B and D, *B. burgdorferi ospA* DNA copies are normalized to copies of the mammalian *Rpp30* gene and p-values are generated by one-way ANOVA on log transformed data with Dunnett's multiple comparison test. For panels A-D, all rodents were between 8-12 weeks old at time of infection and both sexes are present. Figure broken down by sex included as **Figure S1A, S1B**. Bars represent the mean, dots represent individual rodents, and error bars represent the standard error of the mean. (E) *B. burgdorferi* has different population dynamics in ear tissue from *P. leucopus* or *M. musculus* (n=3) following tick bite. Five infected nymphal *I. scapularis* were placed in a tick containment chamber on each rodent's back and ear punches were taken weekly starting at 1.5 weeks post tick placement for ddPCR analysis. P-value generated by two-way ANOVA. For panel E, only male rodents were used and all *M. musculus* were between 8 and 12 weeks old at time of infection while *P. leucopus* were estimated to be equal to or less than six months old. For all panels, data are pooled from two independent experiments.

Examining *B. burgdorferi* and *P. leucopus* interactions over time

To better understand how *P. leucopus* and *B. burgdorferi* B31 interact with each other over the course of infection, we infested 20 *P. leucopus* with infected nymphs and 4 *P. leucopus* with uninfected nymphs across two independent experiments. Each rodent was euthanized at one of five terminal time points (1-, 2-, 4-, 8-, or 13-weeks post infestation, two rodents euthanized per time point per experiment, two independent experiments) to obtain ear and heart tissue for microbiological, genomic, transcriptomic, and histopathological analysis **(Figure 2A)**. Rodents infested with uninfected nymphs were harvested one week post placement. Additionally, each infected rodent was subjected to one intermediate time point (1-, 2-, 4-, 10-weeks post infestation) in which an ear punch was taken from a living rodent prior to infestation with larval *I. scapularis*. These time points were chosen because the spring *I. scapularis* nymphal peak when many *P. leucopus* first get infected and the summer larval peak where larvae can acquire the infection are separated by about 1-3 months [29-31], and thus this captures the most important period of time that *B. burgdorferi* must exist in *P. leucopus* during the enzootic cycle.

To contextualize these results, we repeated these time courses with C57BL/6J and C3H/HeN *M. musculus*. However, it should be noted that due to logistical constraints, these time courses were completed separately and thus caution should be used when directly comparing the *P. leucopus* and *M. musculus* data. Note that this means the same 24 *P. leucopus*, C57BL/6J, or C3H/HeN (total 72 rodents) were used for Figures 2, 3, 4, & 5—with the exact sample size per panel listed in the figure legend.

At each terminal time point, we attempted to culture spirochetes out from approximately one half of a rodent ear in BSK-II. Surprisingly, we were unable to culture *B. burgdorferi* B31 from *P. leucopus* until late in the infection **(Figure 2B)**. This contrasts with our studies with laboratory mouse strains in which *B. burgdorferi* B31 were readily cultured from ears at two weeks post infestation **(Figure 2C)**. Of note, we do observe overall lower and more variable rates of culture positivity than some laboratories have reported using laboratory mice (example [32]) for *Peromyscus* species [15, 28]. The source of this variability is unclear, but our ability to consistently culture *B. burgdorferi* from back tissue following infection and from *M. musculus* at two weeks post infestation leads us to conclude that our culture data are a reliable proxy for large, healthy numbers of spirochetes in tissue, though perhaps a less accurate binary measurement of infectivity. Using a ddPCR threshold of 1 copy of *ospA* DNA per 10,000 copies of *Rpp30*, we observed 100% infectivity in *M. musculus* by two weeks post infection and in *P.*

leucopus by four weeks post-infestation **(Figures 2D, 2E).** Quantification of bacterial burdens corroborated our previous observations **(Figure 1E)** in that *P. leucopus* had a very modest spike in bacterial burden at four weeks post infestation **(Figure 2F)** while both lab mouse strains had substantially higher peaks at two weeks post infestation **(Figure 2G)**. Together these data confirm and expand our conclusions from Figure 1, specifically that *P. leucopus* appear to harbor smaller numbers of *B. burgdorferi* in skin relative to inbred *M. musculus* strains.

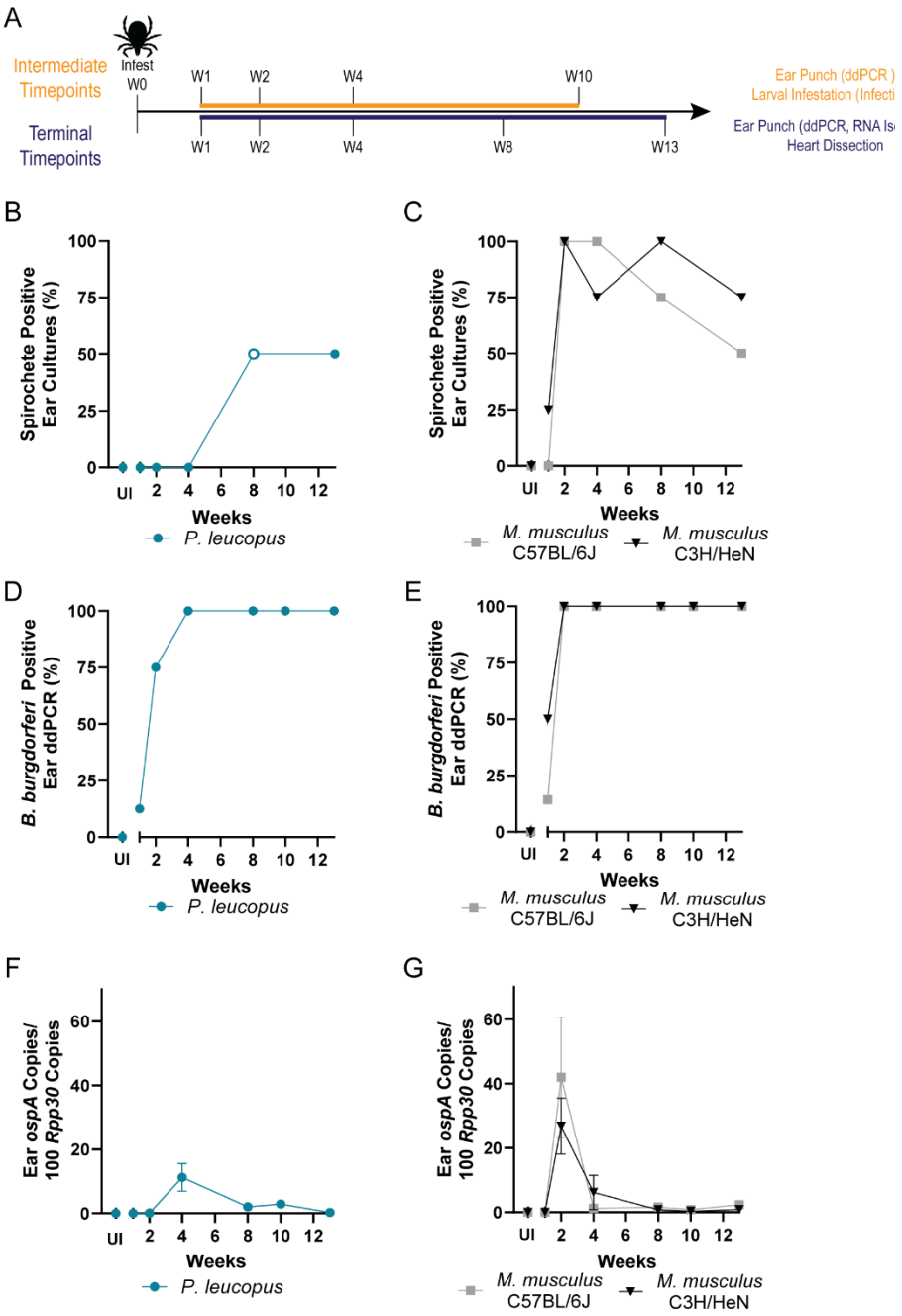

Figure 2: *B. burgdorferi* B31 have different population dynamics in *P. leucopus* and *M. musculus* over thirteen weeks. (A) Schematic of the experimental design used for Figures 2-5. Rodents were infested with five nymphal ticks (infected or uninfected) in a tick containment chamber and harvested at the listed terminal time points. Rodents were subjected to a maximum of one intermediate time point. All rodents were between 6 and 12 weeks old at the time of infection. Each time point included one male and one female rodent per species per experiment where possible. All time points represent between three and eight samples per summarized point depending on if the time point combines terminal and intermediate values (*e.g.* week 2 n=8, week 8 n=4) and/or whether samples needed to be excluded for technical reasons (*e.g.,* rodent death, failed DNA extraction). (B, C) *B. burgdorferi* can be cultured from *P. leucopus* ear punches late in infection (B), while *M. musculus* can be cultured from ear punches starting at two weeks post nymph placement (C). The open circle at eight weeks in panel B represents a contamination issue that prevented us from accurately determining positivity in two of our four cultures. Thus, the appropriate interpretation of this timepoint is that at least half the cultures were positive for spirochetes. (D, E) *B. burgdorferi* can be detected by ddPCR in *P. leucopus* (D) and *M. musculus* (E) ears for most of the infection. A threshold of 1 copy of *ospA* DNA per 10,000 copies of *Rpp30* was selected to distinguish between positive and negative samples. (F, G) *B. burgdorferi* has different population kinetics in *P. leucopus* (F) and *M. musculus* (G) ears as measured by ddPCR. The *B. burgdorferi ospA* gene copies are normalized to copies of the mammalian *Rpp30* gene. Dots represent the mean, error bars the standard error of the mean. Figure broken down by sex included as **Figure S1B**.

P. leucopus are infectious for a shorter period of time than *M. musculus*.

As *P. leucopus* are one of the primary North American reservoirs of *B. burgdorferi* [8], we hypothesized that despite lower abundance of *B. burgdorferi* B31 in *P. leucopus* skin, the bacteria would still efficiently pass the spirochete to larval ticks. To test this hypothesis, we infested rodents in our time course **(Figure 2A)** with larval ticks at intermediate time points. Notably, we also collected ear punch biopsies from the rodents in order to calculate bacterial burden for each specific rodent at the time of infestation.

P. leucopus can transmit infection very soon after placement of infected nymphal ticks with ~25% of larval ticks placed one week after infected nymph feeding yielding viable *B. burgdorferi* B31 **(Figure 3A)**. This increased to 80% at two weeks post nymph placement before sequentially dropping for the duration of the experiment. Notably there was no correlation between the observed bacterial burden in the ear by ddPCR and the proportion of infected larvae recovered from the rodents **(Figure 3B)**. These data together may suggest that in addition to having smaller numbers of viable *B. burgdorferi* B31 in ear, *P. leucopus* may have additional mechanisms that inhibit the spread of *B. burgdorferi* to ticks.

Examining rodent-to-tick transmission in laboratory mouse strains revealed a substantially different pattern. In C57BL/6J mice, ~70% of larvae became infected when placed one week after nymph placement, 100% were infected when placed after two weeks, and >90% were infected when placed thereafter **(Figure 3C**). Similar to *P. leucopus*, there was no relationship between the bacterial burden in the ear and infectivity **(Figure 3D)**. Curiously, while C3H/HeN mice had very similar results to C57BL/6J mice in terms of infectivity kinetics **(Figure 3E)**, we did actually observe a correlation between the burden in ear and infectivity ($p=0.001$, $R^2=0.5755$; Pearson Correlation). This aligns with a recent study which found a relationship between ear burden and larval infectivity in C3H/HeJ mice [33]. Regardless, these data collectively demonstrate that the inbred *M. musculus* strains used here pass *B. burgdorferi* B31 to ticks better and over longer periods of time than *P. leucopus*.

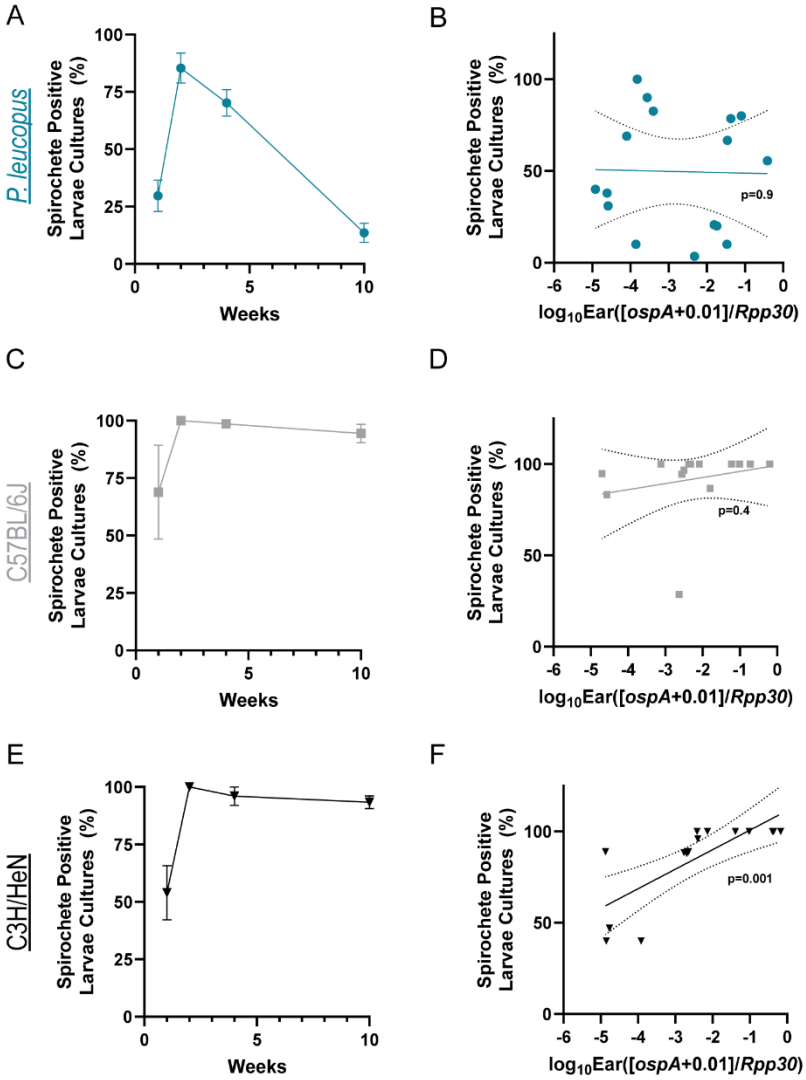

Figure 3: *P. leucopus*, but not *M. musculus*, infected with *B. burgdorferi* B31 become substantially less infectious over time. (A) *P. leucopus* are less infectious over time. Rodents were infested with approximately 50 larval *I. scapularis* at 1, 2, 4, and 10 weeks post-infestation. Larvae were collected 3-4 days later and incubated at room temperature in a humidified chamber for one week before being crushed in BSK-II. Cultures were monitored for three weeks to determine the rate of infectivity from the rodents to *I. scapularis.* (B) In *P. leucopus*, *B. burgdorferi* burden in the ear (measured by ddPCR) does not correlate with infectivity. Ear punches were taken just before infestation with larval ticks. (C, D) C57BL/6J mice remain highly infectious over time (C) and burden in the ear (measured by ddPCR) does not correlate with infectivity (D). (E, F) C3H/HeN mice remain highly infectious over time (E) and burden in the ear (measured by ddPCR) does correlate with infectivity (F). For panels A, C, D, the infectivity was calculated as the number of ticks that yielded culturable spirochetes divided by the total number of ticks collected (5-30 ticks per rodent were collected, average=20.5 ticks/rodent). Rodents with fewer than 5

ticks collected were excluded. Each dot is the mean of 3-4 rodents and the error bar is the standard error of the mean. For panels B, D, F, each dot is an individual rodent, the error bars mark the 95% confidence interval of the slope, and the p-value is from a Pearson r correlation. Figure broken down by sex included as **Figure S1C**.

***P. leucopus* skin transcriptomics reveal a subtle but prolonged immune response against *B. burgdorferi*.**

We hypothesized that our findings that *B. burgdorferi* B31 has an impaired ability to reach high bacterial burdens in the skin of *P. leucopus* and infect ticks could be the result of this species having a subtle but efficient immune response that limits the pathogen's fitness. To test this hypothesis, we performed RNA-seq on *P. leucopus* ear tissue from 1-, 2-, 4-, and 8-weeks post infestation. Notably, while bulk RNA-seq is a blunt tool which cannot always capture the complexities of an immune response, it is a useful technique to begin probing *P. leucopus* immunity given the small number of validated molecular tools for the species.

Differential expression analysis identified a small number of upregulated and downregulated genes across time points **(Figure 4A-D, Supplemental File 1)**. Because we sought to understand *P. leucopus* pathway regulation in response to infection with *B. burgdorferi* B31 we decided to use a relaxed statistical threshold ($p_{adj} \leq 0.1$) in order to reduce our false negative (Type II error) rate. This analysis revealed 10 differentially expressed genes at one week post infestation, 138 at two weeks, 35 at four weeks, and 26 at eight weeks **(Figure 4E)**. Most of these genes had increased expression in response to infection, which is in line with activation of an immune response. Tracking these differentially expressed genes across the time course of the infection revealed that most genes upregulated at two weeks post infestation did not remain upregulated later during infection **(Figure 4F**). However, many of the genes that were still overexpressed at four weeks post infestation also had high expression at eight weeks. Thus, it appears that after a burst of transcriptomic changes in skin by *P. leucopus* during acute infection, the transcriptomic response to *B. burgdorferi* B31 is refined and sustained into late infection. This level of overlap across time points is not observed across downregulated genes **(Figure 4G)**.

We note a few observations from analysis of individual differentially expressed genes. First, across two weeks, four weeks, and eight weeks post infestation, we observed upregulation of multiple C1q genes, which could lead to increased complement-mediated killing of *B. burgdorferi* at these timepoints. Additionally, we observed high expression of *Cxcl13* at four weeks and eight weeks post infestation, which may suggest resident cells are recruiting additional B cells to the skin to kill invading *B. burgdorferi*. Finally, we observed highly statistically significant ($p_{adj} \approx 10^{-60}$) increased expression of *Slamf9* at four weeks and eight weeks post infestation. Notably, this gene was also one of the top hits from Long *et al.*'s study on differential gene expression in the skin of *P. leucopus* at five weeks post intra-peritoneal *B. burgdorferi* infection [14]. *Slamf9* has been associated with proinflammatory cytokine secretion in macrophages [34] and dendritic cells [35]. This may suggest a role for these cells in mediating late-stage inflammation against *B. burgdorferi* B31 in skin.

We next utilized the Qiagen Ingenuity Pathway Analysis (IPA) pipeline [36] to understand which biological pathways appear to be differentially regulated in *P. leucopus* in response to *B. burgdorferi* B31 infection. Critically, the pathways tested by these tools are

based on signaling pathways in *M. musculus*, which may differ from pathways in *P. leucopus*. Understanding this caveat, we used this tool and identified enrichment of differentially expressed genes in numerous canonical pathways associated with immunity **(Figure 4H)**, including phagocytosis, complement, macrophage activity, and B cell and T cell functions at two weeks, four weeks, and eight weeks post infestation. Notably, none of these pathways were enriched in differentially expressed genes at one week post infestation. The analysis also identified numerous cytokine-induced pathways (including Interleukin 6 (IL6), Tumor Necrosis Factor (TNF), Oncostatin M (OSM), and Interleukin 1 beta (IL1β)) that were enriched in the two-week, four-week, and/or eight-week datasets **(Figure 4I**), as well as some immunity associated transcription factor pathways (including STAT3, NFKB2, and STAT5B) that were enriched in some combination of the datasets **(Figure 4J)**. Note, this does not mean that the cytokine or transcription factor itself is differentially regulated in our dataset, but rather that genes known to be regulated by those upstream regulators are enriched in our dataset. Importantly, the IPA pipeline not only assigns a p-value for enrichment, but also attempts to leverage the direction of effect for each differentially expressed gene to determine whether the predicted pathway is turned on or off. Because of the low number of differentially expressed genes at weeks four and eight this software was unable to generate Z scores for most pathways at these time points, however, even with these limitations the software was able to detect evidence of activated phagosome formation pathways at two weeks, four weeks, and eight weeks **(Figure 4K)**, indicating a strong signal of activated phagocyte populations in the skin of *P. leucopus* following *B. burgdorferi* B31 infection.

Focusing on the two-week timepoint where we see a stronger acute response of *P. leucopus* to *B. burgdorferi* B31, the IPA software was able to detect activation of several immune-relevant pathways including phagosome formation, phagocytosis, pathogen recognition receptor activation, natural killer (NK) cell activation, and interleukin 10 (IL10) signaling **(Figure 4L)**. Examining activation of cytokine triggered pathways, the software detected strong activation of the tumor necrosis factor (TNF), oncostatin M (OSM) pathways, and interferon gamma (IFNγ) pathway (Z score = 1.97) **(Figure 4M)**. Finally, examining transcription factor activated pathways the software found evidence of induction of the T cell transcription factors BHLHE40 and STAT3, and the proinflammatory macrophage transcription factors KLF6 and STAT5B **(Figure 4N)**. The software predicted significant repression of the CEBPB and DLX3 regulated pathways. Together, these data demonstrate that while we observe a small number of differentially expressed genes in the skin of *P. leucopus* following *B. burgdorferi* B31 infection, these genes provide a strong signature of an innate and adaptive immune response against the pathogen.

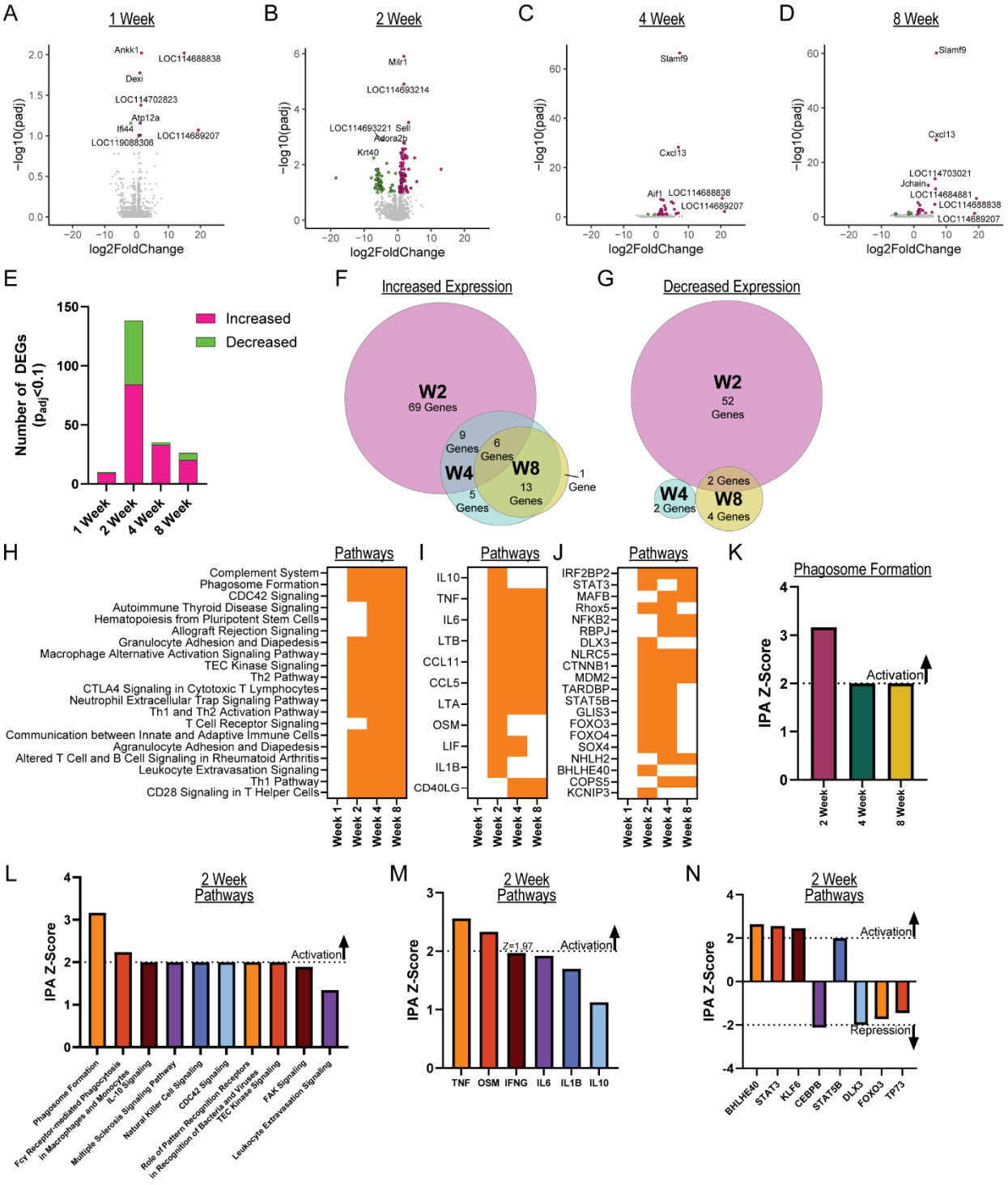

Figure 4: *P. leucopus* have a subtle but prolonged immune response to *B. burgdorferi* B31 in skin. (A-D) Differentially expressed genes in *P. leucopus* skin at 1- (A), 2- (B), 4- (C), and 8-weeks (D) post infestation compared to uninfected *P. leucopus*. Genes with p<0.1 are colored green or pink if down or up regulated, accordingly. (E) More genes are upregulated than downregulated across timepoints using a p<0.1 threshold. (F, G) Many upregulated genes (F) but not downregulated genes (G) overlap across timepoints. Overlap between gene sets was determined using the Biovenn software [37]. (H-N) QIAGEN IPA software [36] reveals enrichment of numerous inflammatory pathways in *B. burgdorferi*-infected *P.*

leucopus. (H-I) Heatmaps show pathways with enrichment for numerous canonical pathways (H), upstream cytokines (I) and transcription factor (J) regulators. Orange boxes represent pathways where enrichment was predicted ($p<0.05$). (K) *P. leucopus* ears at 2-, 4-, and 8-weeks post infestation show activation of phagosome formation pathways. (L-N) At two weeks post infestation, *P. leucopus* ears show evidence of activation of canonical pathways (L), activation of cytokine-triggered pathways (M), and activation and repression of transcription factor-regulated pathways (N). For K-N, activation of pathways was determined using a Z score cutoff of 2 and repression was determined using a Z score cutoff of -2. RNA was derived from 4 *P. leucopus* rodents (two males, two females) at each timepoint.

Inbred *P. leucopus* have very mild carditis following infection

Together, our data demonstrate that *P. leucopus* launch a seemingly robust immune response following infection, leading us to question whether these rodents may display signs of inflammation at the tissue level. While *P. leucopus* are known not to have major behavioral [12, 13] or fitness [10] changes in response to *B. burgdorferi* infection, with one dissenting study noting severe neurological symptoms that correlate with spirochete positivity [38], it remains possible that there are modest physiological changes in response to infection. Close examination of *P. leucopus* histology following infection is surprisingly sparse with some studies have noting a lack of major inflammation in infected adults—though experimentally infected infant *P. leucopus* do develop arthritis [11]. To examine whether *B. burgdorferi* induces an inflammatory response in infected systemic tissues, we collected hearts from our inbred *P. leucopus* and the *M. musculus* strains at the terminal timepoints (**Figure 2A)** for histopathological analysis.

In line with our observations that there is a modest but sustained inflammatory response in long-term infected *P. leucopus* we observed very mild carditis in *P. leucopus* four weeks post infestation **(Figure 5A, File S2)**. This inflammation was substantially lower than what we observed in C3H/HeN mice **(Figure 5B, File S2)** and slightly lower than we observed for C57BL/6J mice **(Figure 5C, File S2)**. This suggests that there is, indeed, a mild but detectable inflammatory response against *B. burgdorferi* B31 in *P. leucopus* hearts. We do briefly note that we attempted to also measure inflammation in *P. leucopus* joints, however, we found that Bouins solution was insufficient to decalcify the bones in the leg, resulting in destruction of our samples.

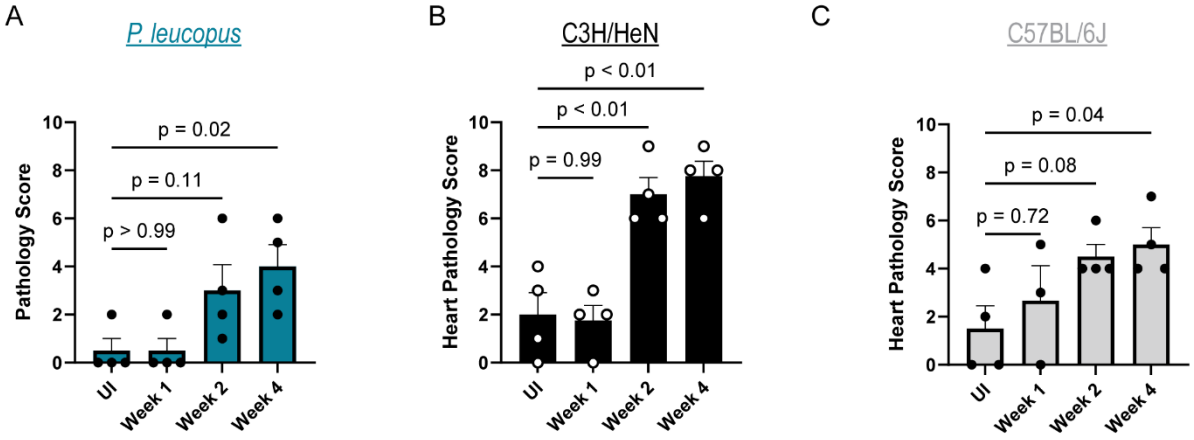

Figure 5: Inbred *P. leucopus* develop very mild carditis following *B. burgdorferi* B31 infection.

Histopathological analysis of hearts from (A) *P. leucopus*, (B) C3H/HeN, and (C) C57BL/6J mice (n=3-4) following infection. Each dot represents the blinded score from a single mouse based on myocarditis, valvulitis, arteritis, and myocardial fibrosis. Subscore for each score component can be found in **File S2**. Dots represent individual mice, bars represent the mean, error bars the standard error of the mean. P-values calculated by one-way ANOVA with Dunnett's multiple comparisons test. Figure broken down by sex included as **Figure S1D**.

Impact of biological sex on phenotypes

For nearly all experiments in this manuscript (with the exception of **Figure 1E**), male and female rodents were used. While the overall small design of these studies make it difficult to dissect the impact of sex on *B. burgdorferi* burden, rodent-to-larvae transmission, and induction of heart pathology, we have included these data stratified by sex in **Figure S1**. We do note a handful of statistically significant findings, even with these small sample sizes (2-4 animals per sex per phenotype), which aligns with previous studies that have noted rodent sex impacts *B. burgdorferi* phenotypes [33, 39]. First, while there was no effect of sex on *B. burgdorferi* B31 burden at the needle injection site **(Figure S1A)** we did find that C3H/HeN male mice have higher burdens at the tick placement site than female mice one week post infestation **(Figure S1B)**. A comparable but non-statistically significant trend was observed for C57BL/6J mice—likely due to the small sample size. There was no statistically significant effect of sex on ear burden over time in the *M. musculus* strains or *P. leucopus* **(Figure S1C)**, though some trends were observed at various timepoints, raising the possibility that further study is warranted. We observed worse transmission of *B. burgdorferi* B31 to larval ticks in female *P. leucopus* at four-weeks post infestation (p=0.08) and C3H/HeN mice at 10 weeks post infestation **(Figure S1D)**, with some similar non-statistically significant trends observed in *P. leucopus* at one week post infestation and C57BL/6J mice at 10 weeks post infestation. No statistically significant sex-biased phenotypes were observed in heart histopathology data **(Figure S1E)**, though there was a notable trend towards female *P. leucopus* having higher inflammation at two weeks post infestation that may warrant further study.

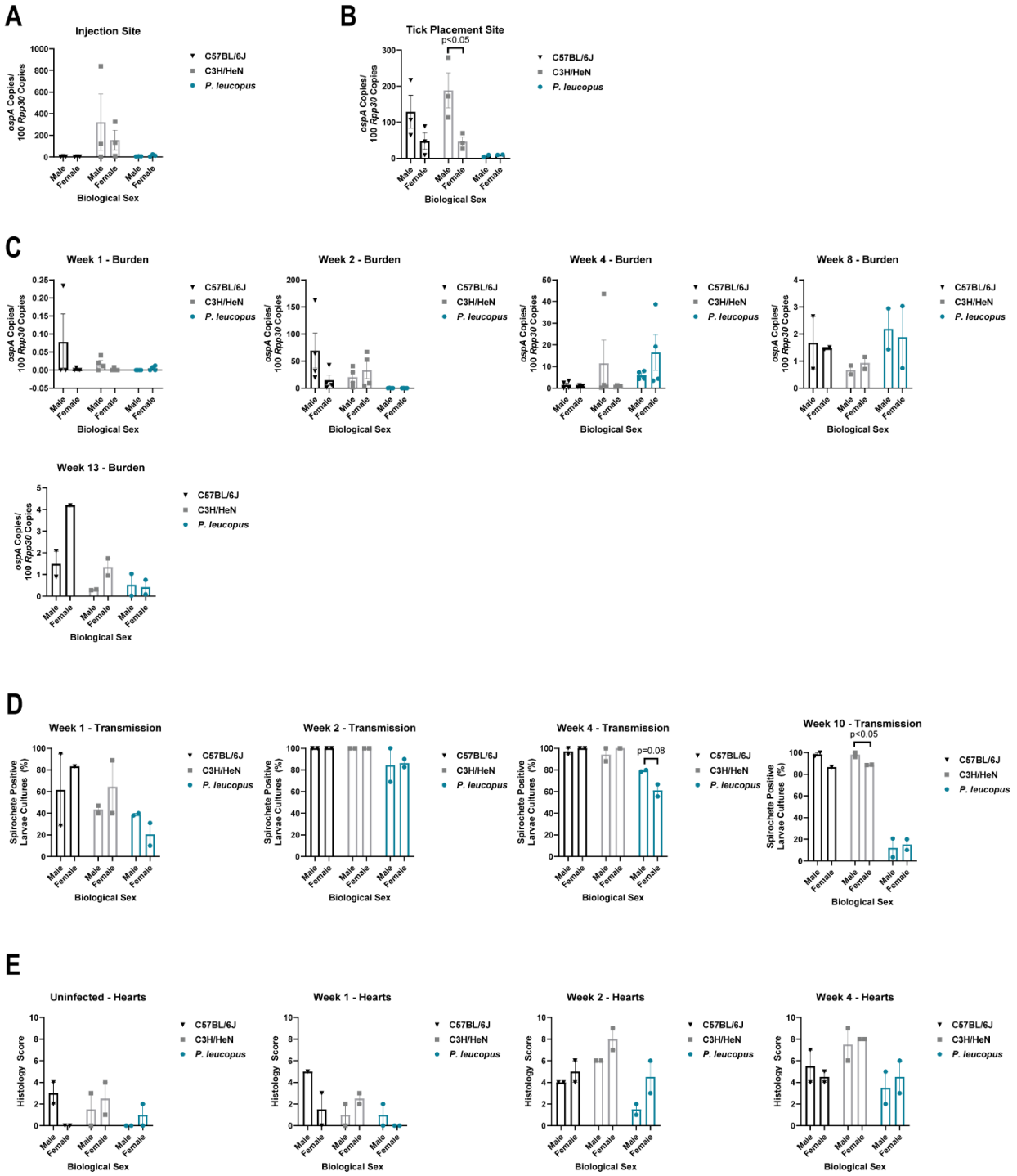

p-values are generated by Student's t-test. Only p-values <0.1 are displayed.
Each dot represents data from a single mouse

Figure S1: Effects of biological sex on *B. burgdorferi* phenotypes.

Data from Figures 1, 2, 3, and 5 broken down by sex, including bacterial burden in the needle injection site (A) and tick placement site (B) one week post infection, and ear tissue (C) during the 13-week timecourse, as well as transmission to larval ticks (D) and histology of the heart (E).

Discussion

The primary goals of this work were to understand (a) how *P. leucopus* respond to infection with *B. burgdorferi* B31, and (b) how this response compares to the traditional *M. musculus* lab mouse model of infection. Historically, the lab mouse has been used to model manifestations of human Lyme disease and as a catch all model of mammalian-*B. burgdorferi*-tick infection kinetics. However, our data suggest that *M. musculus* are a poor mimic of *P. leucopus*-*B. burgdorferi* interactions, as *B. burgdorferi* B31 has dramatically different infection kinetics in the two systems and have reduced capacity to infect larval *I. scapularis* in inbred *P. leucopus*. While *M. musculus* and muroids can serve as competent hosts for *B. burgdorferi*—particularly in Europe—North American *B. burgdorferi* strains predominantly coexist with *P. leucopus* and shrews [8], and thus we were surprised to observe this elevated *B. burgdorferi* B31 (a North American strain) fitness in the *M. musculus* non-native hosts. We consider these results to be counter intuitive as we anticipated that the ability for *B. burgdorferi* to sustain in nature would have depended on potent and sustained susceptibility of *P. leucopus* to *B. burgdorferi* infection across all strains—including B31.

We note that we are not the first group to attempt to measure experimentally infected *P. leucopus* transmission of *B. burgdorferi* to *I. scapularis*, and indeed our measurements of infectivity align with prior observations using the JD1 strain of *B. burgdorferi* [16], but curiously diverged substantially from a recent report which used the B31-5A4 clonal strain and found larval infectivity increased over the first five weeks of infection before slightly dropping eight weeks post infection [19]. We note that in this latter report qPCR was used to detect *B. burgdorferi* rather than the culture-based methods used here. We speculate that the use of PCR may have overreported the abundance of infected ticks. Notably our results did more closely match with previous studies using B31 in *P. maniculatus* [28] and another OspC Type A strain (BL206) or a Type C strain (B348) in *P. leucopus* [17], both of which used PCR based detection methods to confirm infection. Curiously, while the latter study had slightly higher infectivity of BL206 in *P. leucopus* than we observed with B31, they actually saw substantially worse infectivity in C3H mice over time than we did across similar timescales. This likely demonstrates that there is natural genetic diversity within OspC types that influences vertebrate to tick transmission. Supporting this, analysis of additional strains across the literature have found highly variable patterns in rodent (*P. leucopus* [40-42] or C3H *M. musculus* [33, 43]) to *I. scapularis* transmissibility over time.

These data highlight a major limitation and important future direction of this work, which is that we only tested our findings with the B31 *B. burgdorferi* strain. We chose B31 (originally derived from a North American tick [44]) because it is the most commonly used laboratory strain and the genomic type strain of *B. burgdorferi* and, as such, our results would be comparable to other studies using this strain in *M. musculus*. Recent work Zinck *et al*. has emphasized that there are substantial differences among *B. burgdorferi* strains in their ability to infect ticks from C3H/HeJ mice [33], raising the possibility that other strains may be better or worse adapted to *P. leucopus*. In line with this, there is evidence of strain specificity within different reservoir hosts [19, 45, 46]. Screening additional *B. burgdorferi* strains in *P. leucopus* could enable identification

of variable spirochete loci that associate with higher transmission. Understanding the impacts of those theoretical spirochete loci on transmission from other vertebrate hosts could broaden our understanding of *B. burgdorferi* evolution. It will also be interesting to examine whether genotypes that associate with enzootic spread align with loci that associate with disease severity in the dead-end human host [47].

We have five non-mutually exclusive hypotheses that could explain our findings that our inbred *P. leucopus* harbor smaller *B. burgdorferi* B31 populations and are less infectious that C57BL/6J or C3H/HeN mice, First, it is possible that *B. burgdorferi* is not under selection to reach high levels of infection or infectivity in nature, as the sheer number of *P. leucopus* and *I. scapularis* in North America mean even a mildly successful mammalian infection results in reproductive success from the bacteria's perspective. Given the number of selective pressures *B. burgdorferi* faces across the enzootic cycle, including cycling into and out of a range of vertebrate hosts beyond *P. leucopus*, it's possible that this represents a "hedged" strategy in which *B. burgdorferi* can infect numerous hosts to various degrees while selection ensures only that the spirochete remains at least partially infectious in the *P. leucopus* host. This is supported by data that the *ospC* genotype (Genotype A) of B31 is associated with a generalist lifestyle [46, 48]. We may have observed substantially better infection and transmission if we had infected with a strain with *ospC* Type K, which appears to be a *B. burgdorferi* clade more closely associated with *P. leucopus* infection [19, 46].

Second, as field studies have observed high *Peromyscus* to *I. scapularis* transmission in nature (>90%) [49], wild *P. leucopus* may be better suited to spread *B. burgdorferi* to ticks. This may result from "immunosuppression" resulting from environmental conditions (food stress, co-infections, pregnancy) that are absent in the laboratory [50, 51]. Third, our data could support that there is a tradeoff of how densely abundant the bacteria remain in the host, how easily individual bacteria transmit, and how fit the host remains over time. Fourth, while the peaks of nymphal and larval *I. scapularis* density are often represented as being separated by seasons (~1-3 months depending on site), there is a range of time where both larvae and nymphs can be found in the environment [29-31]. Therefore, it's possible that a substantial amount of *P. leucopus* to *I. scapularis* larvae transmission occurs during the first month of infection when we still observe high rates of infectivity.

While the above hypotheses may explain the lower-than-expected *P. leucopus* infectivity, they do not explain the higher-than-expected reservoir competence in the non-native host *M. musculus.* Our fifth explanation that addresses this finding is that the specific inbred *M. musculus* strains selected here may be particularly permissive to *B. burgdorferi* B31 transmission, which could make sense as our B31 strain (B31-AD) is routinely passaged in C57BL/6J or C3H/HeN mice to preserve pathogenicity. Inter-rodent strain variability has long been noted for susceptibility to arthritis [52, 53] and thus it is very possible that variation in *M. musculus* reservoir competency also exists. Additionally, as there are approximately 25 million years of divergent evolution between *P. leucopus* and *M. musculus* [54], it may also be interesting to compare *P. leucopus* with a more closely-related model organism such as hamsters, which are competent hosts [55], to better examine how unique the relationship is between *P. leucopus* and *B. burgdorferi*.

We found that *B. burgdorferi* nucleic acid copy numbers in ear largely did not correlate with larval tick infectivity, with the exception of when ticks are fed on C3H/HeN mice. While this latter finding matches recent work that demonstrated a relationship between burden in ear biopsies and tick infectivity using C3H mice [33], it raises questions about why this was not observed for C57BL/6J mice or *P. leucopus*. One explanation is that ear biopsies are not representative of overall skin burden [33, 39], or that their strength as a representative tissue differs across species and strains. In particular this could explain why C57BL/6J mice had such high levels of transmission one week post nymphal infestation when *B. burgdorferi* were still largely undetectable in ear. A non-mutually exclusive hypothesis is that perhaps there are soluble mechanisms of diminishing transmission to ticks via the bloodmeal in *P. leucopus*—explaining the lower-than-expected transmission when skin burdens are high. Indeed, there is some precedent for this as antibody and/or complement have been shown to kill *B. burgdorferi* in larval ticks fed on *ospA* vaccinated *M. musculus* [56, 57]. We speculate that development of natural anti-*Borrelia* immunity may more potently enable antibody and/or complement to kill escaping *B. burgdorferi* B31 in *P. leucopus* compared to C57BL/6J or C3H/HeN mice.

In our RNA-sequencing dataset, similar to a past transcriptomic study [14], we note limited direct evidence of immunity (*e.g.* a large number of differentially expressed cytokines), which can likely be attributed to the relatively small number of infiltrating immune cells into the large numbers of epithelial and mesenchymal cells that make up the tissue. However, based on our data examining *B. burgdorferi* fitness during the acute stages of *P. leucopus* infection, we hypothesize that the immune response we detect here is extremely efficient and contributes to limiting *B. burgdorferi* infection. Curiously, while we observed overlap of increased *Slamf9* expression in *B. burgdorferi*-infected *P. leucopus*, this represents one of only a few similarities between our work and the study of Long *et al*. [14]. We note numerous differences in the experimental design that may account for disparities between the studies: (1) differences in infection method (intra-peritoneal vs nymph), (2) differences in *B. burgdorferi* strain (Sh-2-82 vs B31), and (3) differences in *P. leucopus* source (LL Stock from the Peromyscus Genetic Stock Center vs the Tufts University Peromyscus Colony). Dissecting the impacts of these variables on *P. leucopus*-*B. burgdorferi* interactions remains an important future direction. Current work is also focused on comparing the differentially expressed genes in *P. leucopus* skin following infection to those that are differentially expressed in *M. musculus*. For instance, comparing our dataset to a single cell RNA-sequencing dataset generated on C57BL/6J ankles [58] revealed that while we observe high *Cxcl13* expression late in infection in *P. leucopus* skin, it is associated only with early infection in *M. musculus* ankles. Further mining of these datasets may provide insight into why *M. musculus*, but not *P. leucopus,* harboring *B. burgdorferi* B31 remain infectious to larval ticks over long periods of time.

Of note, while we specifically examined how readily *B. burgdorferi* transmits from rodents to larval *I. scapularis*, survival of the bacteria until the tick has successfully molted and is ready to feed again is critical for the enzootic cycle. Therefore, future work should specifically address how readily *B. burgdorferi* from different hosts survive in ticks to complete the cycle. While our intuition is that we expect somewhat lower rates of infected ticks following the molt, some work has suggested that it may actually be easier to detect *B. burgdorferi* from flat nymphs than recently repleted larvae [33]. Comparing the detectability of *B. burgdorferi* in recently fed larvae, seven-day repleted larvae (as performed here), and flat nymphs after

feeding on different reservoir hosts may reveal interesting biology that occurs during the *I. scapularis* stages of the *B. burgdorferi* life-cycle.

In sum, our data demonstrate that the infection, spread, and control of *B. burgdorferi* follow dramatically different rules in *P. leucopus* than *M. musculus*. This highlights a tried-and-true principal of experimental design borrowed from the statistician George E. P. Box: "All models are wrong, but some are useful." Here we propose that while *M. musculus* are a useful model for many aspects of *B. burgdorferi* infection, they may not accurately model the North American enzootic cycle. We hope that improving our understanding of how *P. leucopus* limit spread of *B. burgdorferi* B31 into new hosts could provide new insights into controlling *B. burgdorferi* abundance in nature through reservoir targeted interventions.

Acknowledgements

The authors would like to thank Dr. Alan Barbour for numerous helpful conversations over the course of this project. RNA sequencing analyses were made possible by the Tufts High Performance Computing Cluster (https://it.tufts.edu/high-performance-computing). We thank past and present members of the Hu lab for helpful feedback during the formulation of this project and in assisting with the bioinformatic analyses, particularly Julie McCarthy and Peter Gwynne.

Methods

Bacterial culture

Borrelia burgdorferi strain B31 (Hu Lab AD strain, routinely reisolated from sequential passages through C3H/HeN mice after obtaining the parental strain from Patricia A. Rosa) was cultured in Barbour-Stoenner-Kelley II (BSK-II) medium in stationary, sealed tubes at 32°C until mid-exponential phase growth (~$5x10^7$ spirochetes/mL). BSK-II was made according to existing protocols (Table 2, [59]) and quality controlled by confirming *B. burgdorferi* growth was unaffected across batches. Bacteria were monitored for growth, motility, and counted by pairing a Petroff-Hausser counter with darkfield microscopy. B31-AD stocks were passaged a maximum of one time *in vitro* following isolation from subcutaneously infected C3H/HeJ (Jackson Labs, Strain: 000659) skin two to four weeks post-infection in order to generate frozen stocks in 25% glycerol. Plasmid content was measured after thawing from frozen stocks. In order to limit environmental contamination when culturing spirochetes from rodent or tick tissue, phosphomycin disodium (100µg/mL, Sigma P5396), rifampicin (50µg/mL, Sigma R3501), and amphotericin B (5µg/mL, Sigma A4888) were added to the medium. Cultures from tissue were monitored weekly by darkfield microscopy and cultures were considered positive if spirochetes were observed within three weeks of culture start.

Table 1: BSK Reagent List

Product	Manufacturer	Product #	Amount (grams) per 2000mL Water
CMRL with L-glutamine	US Biologics	C5900	19.3
Neopeptone	BD	211681	11.1
Yeastolate	Gibco	255772	4.44

Hepes acid	Fisher	BP310-100	13.32
Dextrose	Fisher	BP350-500	11.1
Sodium citrate	Fisher	S279-500	1.55
Sodium pyruvate	Fisher	BP356-100	1.78
N-acetyl-glucosamine	ThermoFisher	A13047.18	0.89
Sodium bicarbonate	Fisher	BP328-500	4.88
Gelatin B	Acros Organics	61225-5000	1.06% Final Concentration (~400mL of a 7% autoclaved solution)
Rabbit serum (Heat Inactivated)	Gibco	16120-099	5% Final Concentration (~131mL)
BSA	Millipore Sigma	810037	5% Final Concentration
Sodium Hydroxide			To pH 7.6

Rodent Maintenance, Use, and Ethical Statement

All animal procedures were approved by the Tufts University-Tufts Medical Center Institutional Animal Care and Use Committee (IACUC, Protocol #B2021-84). Euthanasia was performed in accordance with guidelines provided by the American Veterinary Medical Association (AVMA) and was approved by the Tufts University IACUC. Rodents were maintained by the Tufts Comparative Medicine Services. The inbred *P. leucopus* colony was started by Dr. Sam Telford using wild captured rodents from the northeastern and midwestern United States. The colony has been closed since 1994, held in microisolator cages, and is specific pathogen free (regular sentinel testing).

With the exception of **Figure 1E**, all rodents were between 7 and 12 weeks old at the time of infection. Experiments were started with equal numbers of male and female rodents. Sample sizes are included in the figure legends for each panel. For **Figure 1E**, only male rodents were used and *P. leucopus* were >3 months and <10 months old, while both *M. musculus* strains were between 7 and 12 weeks old. No rodents were excluded from analysis unless either (1) unexpected rodent death or (2) failed nucleic acid extraction) prevented data collection.

Generation of *Ixodes scapularis* Nymphs

Immunocompromised C3H *scid* mice (C3SnSmn.Cg-Prkdcscid/J, Jackson Labs, Strain: 001131) were infected by subcutaneous injection of $1x10^5$ *B. burgdorferi* in 200 µL of BSK-II media. Two to eight weeks post-infection rodents were infested with larval *I. scapularis* (National Tick Research and Education Resource, Oklahoma State University, stored at 4°C in airtight containers containing saturated potassium sulfate). To infest rodents, ~100 larval ticks were placed in modified 50 mL conical tube prior to placing a rodent in the tube. Rodents were restrained with ticks for one hour before returning to a cage suspended in a water moat. Water moats were monitored for ten days to collect fed larval ticks. Up to 6 fed larval ticks were stored in 1.7 mL microcentrifuge tubes with needle-generated airholes in an airtight glass desiccator

containing water, allowed to molt, and stored for between 10 to 52 weeks post larval feeding. For each batch of nymphal ticks, six molted nymphs were crushed in BSK-II and monitored for spirochetes to confirm infection—and all six nymphs were consistently found to be infected. Uninfected nymphs were identically generated except for the use of uninfected C57BL/6J (Jackson Labs, Strain: 000664) mice and were confirmed to be uninfected by crushing in BSK-II.

Rodent Infection with *B. burgdorferi*

Mus musculus (C57BL/6J [Jackson Labs, Strain: 000664], C3H/HeN [Charles River Laboratories, Strain: 025]) and *Peromyscus leucopus* (Sam Telford, Tufts University) were shaved prior to infection. The *P. leucopus* colony has been inbred since 1994 and have been maintained under specific pathogen-free conditions. For needle infections, 200 µL of BSK-II containing $1x10^5$ bacteria were subcutaneously injected into each rodent at a dorsal posterior site. For nymph placements, a 1:4 mixture of melted beeswax to rosin gum mixture was heated and used to attach the top of a modified 1.7 mL microcentrifuge tube lined with mesh between the shoulder blades of the rodent. Five nymphal ticks were carefully placed through the mesh and into the placement cap. Four days later, caps were carefully removed, and ticks were collected. Rodents were singly housed in cages suspended in a water moat until all ticks were collected. Rodents were then returned to cohabitation with other infected animals of the same strain and sex.

Determining Bacterial Burden

DNA from ears was collected by taking one to two 2-mm ear punches from one or both ears at listed time points. DNA from the tick bite or needle site was collected by dissection of a roughly 2 mm region in the center of the shaved region. In all cases, DNA was extracted using the Qiagen Blood and Tissue kit following overnight incubation at 56°C in Buffer ATL with Proteinase K. Following DNA extraction, digital droplet PCR (ddPCR) was performed to quantify the amount of *B. burgdorferi* DNA relative to rodent DNA. Primer probe pairs targeting mammalian *Rpp30* or *B. burgdorferi* are listed in **Table 2**. The primers targeting *Rpp30*, located, are predicted to produce only a single product per gene copy per haplotype in both *Mus musculus* (Chromosome 19) and *Peromyscus leucopus* (Chromosome 1) [14, 60]. Briefly, the Bio-Rad ddPCR Supermix for Probes (no dUTP) kit was used to perform the reaction within droplets generated by the QX200 droplet generator (Bio-Rad) in Oil-for-Probes (Bio-Rad). The reaction included 10 minutes at 95°C, 40 cycles of 94°C for 30 seconds and 60°C for 1 minute, followed by 10 minutes at 98°C and cooling to 4°C for at least 30 minutes to stabilize droplets. Fluorescence was calculated by the QX200 droplet reader and analyzed on the QX Manager Software (Bio-Rad).

Table 2: Oligonucleotides used in this study

Target	Forward	Reverse	Probe
Mus musculus Rpp30	CCAGCTCCGTTTGTGATAGT	CAAGGCAGAGATGCCCATAA	CTGTGCACACATGCATTTGAGAGGT (5'HEX, 3'Iowa Black FQ)
Peromyscus leucopus Rpp30	CTTAGCTCCCGCTTGTTTCT	AAACCTGGTAAGCCAGTGTC	ACACACTTTCTCCTCTTCTTGCTGCA (5'HEX, 3'Iowa Black FQ)

B. burgdorferi ospA	ATGTTAGCAGCCTTGACGAG	TCGTACTTGCCGTCTTTGTT	AGCGTTTCAGTAGATTTGCCTGGTG (5'6-FAM, 3'Iowa Black FQ)

RNA Extraction and Sequencing

One 2-mm ear punch from each ear was collected and submerged in RNA-later (Invitrogen) overnight at room temperature before being frozen at -80°C. After all samples were collected, samples were thawed on ice, transferred to QIAzol, and bead beaten with a 6.35 mm chrome steel bead (Biospec Products) for two cycles of two minutes each at an oscillation frequency of 30/second using a TissueLyser II (Qiagen). RNA was extracted using the miRNeasy mini kit (Qiagen), with the modification that two RWT washes were performed. gDNA was digested using TURBO DNase (Invitrogen) and RNA was repurified using the RNeasy MinElute Cleanup Kit (Qiagen). Purified RNA was submitted to Azenta Life Sciences/Genewiz for library preparation and sequencing (Illumina HiSeq 2x150bp).

RNA Sequencing Analysis

Reads were aligned to the *P. leucopus* genome (GCF_004664715.2) [14] using STAR version 2.6.1 [61] and gene expression was summarized using RSEM version 1.3.1 [62]. All differential gene expression analyses were performed with R (version 4.3.1) using DESeq2 version 1.40.2 [63] using standard parameters. Only genes with ≥10 reads across all conditions (summed) were included in the analysis. Differential gene expression was calculated by comparing to uninfected rodents (rodents that were infested with uninfected nymphs and harvested one week later) and adjusted p-values were based on a calculated false discovery rate. Additional pathway analysis was performed with the use of QIAGEN IPA (QIAGEN Inc., https://digitalinsights.qiagen.com/IPA) [36] using genes with an adjusted p-value cutoff of <0.1.

Determining Transmission from Rodents to Larval *Ixodes scapularis*

At each timepoint ~50 larval ticks were placed in modified 50 mL conical tube prior to placing a rodent in the tube. Rodents were restrained with ticks for one hour before returning to a cage suspended in a water moat. Water moats were monitored at days three and four to collect fed larval ticks. Between 5 and 30 fed larvae were collected per rodent and stored in an airtight glass desiccator containing water for one week to enable *B. burgdorferi* replication in the bloodmeal. Ticks were submerged in 70% ethanol and each tick was crushed in 1 mL of BSK-II containing phosphomycin (100 µg/mL), rifampicin (50 µg/mL), and amphotericin B (5 µg/mL). Cultures were grown at 32°C, monitored weekly by darkfield microscopy, and cultures were considered positive if spirochetes were observed within three weeks of culture start.

Histological Analysis

Whole hearts were fixed in Bouin's fluid (Sigma-Aldrich), then bisected longitudinally and both halves paraffin embedded. Tissues were then sectioned and stained with hematoxylin and eosin (H&E; Cancer Diagnostics Inc) at the Comparative Pathology and Genomics Shared Resource at the Tufts Cummings School of Veterinary Medicine. Slides were blindly scored for myocarditis, valvulitis, arteritis and periarteritis, and myocardial fibrosis by a veterinary anatomic pathologist at Tufts as described below and an overall score (up to 10) was calculated for each animal. Specific definitions score criteria are defined as follows: **Myocarditis** [0 = no inflammation or occasional (≤3) clusters of 1-2 leukocytes (lymphocytes, histiocytes, or neutrophils) at the region of heart base (ventricular and atrial myocardium and epicardium; 1 =

1-2 clusters of 3+ leukocytes; 2 = 3-4 clusters of 3+ leukocytes; 3 = 5+ clusters of 3+ leukocytes], **Valvulitis** [0 = no inflammation or 1-2 leukocytes (lymphocytes, histiocytes, or neutrophils) within a valve (Valve leaflets and cusps (atrioventricular and semilunar)); 1 = 3-5 leukocytes; 2 = 6-10 leukocytes; 3 = 11+ leukocytes], **Arteritis and Periarteritis** [0 = no inflammation or occasional (≤3) clusters of 1-2 leukocytes (lymphocytes, histiocytes, or neutrophils) in the Aorta and pulmonary artery (tunica intima, media, or adventitia) and periarterial connective tissue; 1 = 1-2 clusters of 3-5 leukocytes; 2 = 3-4 clusters of 3-10 leukocytes or 1 cluster of 11+ leukocytes; 3 = 5+ clusters of 3-10 leukocytes or 2+ clusters of 11+ leukocytes], **Myocardial Fibrosis** [0 = absent in the region of heart base; 1 = present).

Data Availability

Sequencing data are deposited in GEO under accession number GSE244071.

Supplemental Legends

File S1: Results from RNA sequencing performed on *P. leucopus* ear punches.
Results from DESeq2 [63]. Data are from 1 Week Post (tick) Placement (1WPP), 2WPP, 4WPP, and 8WPP compared to ear punches from *P. leucopus* one week post uninfected tick placement.

File S2: Histopathology scores of hearts

Figure S1: Effects of biological sex on *B. burgdorferi* phenotypes.
Data from Figures 1, 2, 3, and 5 broken down by sex, including bacterial burden in the needle injection site (A) and tick placement site (B) one week post infection, and ear tissue (C) during the 13-week timecourse, as well as transmission to larval ticks (D) and histology of the heart (E).

Citations

1. Steere, A.C., T.F. Broderick, and S.E. Malawista, *Erythema chronicum migrans and Lyme arthritis: epidemiologic evidence for a tick vector.* Am J Epidemiol, 1978. **108**(4): p. 312-21.
2. Wallis, R.C., et al., *Erythema chronicum migrans and lyme arthritis: field study of ticks.* Am J Epidemiol, 1978. **108**(4): p. 322-7.
3. Burgdorfer, W., et al., *Lyme disease-a tick-borne spirochetosis?* Science, 1982. **216**(4552): p. 1317-9.
4. Radolf, J.D., et al., *Of ticks, mice and men: understanding the dual-host lifestyle of Lyme disease spirochaetes.* Nat Rev Microbiol, 2012. **10**(2): p. 87-99.
5. Anderson, J.F., et al., *Involvement of birds in the epidemiology of the Lyme disease agent Borrelia burgdorferi.* Infect Immun, 1986. **51**(2): p. 394-6.
6. Kornblatt, A.N., P.H. Urband, and A.C. Steere, *Arthritis caused by Borrelia burgdorferi in dogs.* J Am Vet Med Assoc, 1985. **186**(9): p. 960-4.
7. Levine, J.F., M.L. Wilson, and A. Spielman, *Mice as reservoirs of the Lyme disease spirochete.* Am J Trop Med Hyg, 1985. **34**(2): p. 355-60.
8. Goethert, H.K., et al., *Host-utilization differences between larval and nymphal deer ticks in northeastern U.S. sites enzootic for Borrelia burgdorferi sensu stricto.* Ticks Tick Borne Dis, 2023. **14**(6): p. 102230.
9. Bunikis, J., et al., *Borrelia burgdorferi infection in a natural population of Peromyscus Leucopus mice: a longitudinal study in an area where Lyme Borreliosis is highly endemic.* J Infect Dis, 2004. **189**(8): p. 1515-23.
10. Hofmeister, E.K., et al., *Longitudinal study of infection with Borrelia burgdorferi in a population of Peromyscus leucopus at a Lyme disease-enzootic site in Maryland.* Am J Trop Med Hyg, 1999. **60**(4): p. 598-609.
11. Moody, K.D., et al., *Experimental Borrelia burgdorferi infection in Peromyscus leucopus.* J Wildl Dis, 1994. **30**(2): p. 155-61.
12. Wright, S.D. and S.W. Nielsen, *Experimental infection of the white-footed mouse with Borrelia burgdorferi.* Am J Vet Res, 1990. **51**(12): p. 1980-7.
13. Schwanz, L.E., et al., *Borrelia burgdorferi has minimal impact on the Lyme disease reservoir host Peromyscus leucopus.* Vector Borne Zoonotic Dis, 2011. **11**(2): p. 117-24.
14. Long, A.D., et al., *The genome of Peromyscus leucopus, natural host for Lyme disease and other emerging infections.* Sci Adv, 2019. **5**(7): p. eaaw6441.
15. Gaber, A.M., et al., *Comparative transcriptome analysis of Peromyscus leucopus and C3H mice infected with the Lyme disease pathogen.* Front Cell Infect Microbiol, 2023. **13**: p. 1115350.
16. Donahue, J.G., J. Piesman, and A. Spielman, *Reservoir competence of white-footed mice for Lyme disease spirochetes.* Am J Trop Med Hyg, 1987. **36**(1): p. 92-6.
17. Hanincova, K., et al., *Fitness variation of Borrelia burgdorferi sensu stricto strains in mice.* Appl Environ Microbiol, 2008. **74**(1): p. 153-7.
18. Trager, W., *Living Together The Biology of Animal Parasitism*. 1986, New York: Springer New York.
19. Lin, Y.P., et al., *Cellular and immunological mechanisms influence host-adapted phenotypes in a vector-borne microparasite.* Proc Biol Sci, 2022. **289**(1969): p. 20212087.
20. Balderrama-Gutierrez, G., et al., *An Infection-Tolerant Mammalian Reservoir for Several Zoonotic Agents Broadly Counters the Inflammatory Effects of Endotoxin.* mBio, 2021. **12**(2).
21. Ana Milovic, J.V.D., Alan G. Barbour, *The white-footed deermouse, an infection tolerant reservoir for several zoonotic agents, tempers interferon responses to endotoxin in comparison to the mouse and rat.* eLife, 2023. **12**(RP90135).

807 22. Wang, X., et al., *Relative contributions of innate and acquired host responses to bacterial control*
808 *and arthritis development in Lyme disease.* Infect Immun, 2005. **73**(1): p. 657-60.
809 23. Miller, J.C., et al., *A critical role for type I IFN in arthritis development following Borrelia*
810 *burgdorferi infection of mice.* J Immunol, 2008. **181**(12): p. 8492-503.
811 24. Zhi, H., J. Xie, and J.T. Skare, *The Classical Complement Pathway Is Required to Control Borrelia*
812 *burgdorferi Levels During Experimental Infection.* Front Immunol, 2018. **9**: p. 959.
813 25. Ma, Y., et al., *Distinct characteristics of resistance to Borrelia burgdorferi-induced arthritis in*
814 *C57BL/6N mice.* Infect Immun, 1998. **66**(1): p. 161-8.
815 26. Lochhead, R.B., et al., *Endothelial cells and fibroblasts amplify the arthritogenic type I IFN*
816 *response in murine Lyme disease and are major sources of chemokines in Borrelia burgdorferi-*
817 *infected joint tissue.* J Immunol, 2012. **189**(5): p. 2488-501.
818 27. Diterich, I., et al., *Borrelia burgdorferi-induced tolerance as a model of persistence via*
819 *immunosuppression.* Infect Immun, 2003. **71**(7): p. 3979-87.
820 28. Rogovskyy, A.S., et al., *Evaluation of the Importance of VlsE Antigenic Variation for the Enzootic*
821 *Cycle of Borrelia burgdorferi.* PLoS One, 2015. **10**(4): p. e0124268.
822 29. Simmons, T.W., et al., *Seasonal Activity, Density, and Collection Efficiency of the Blacklegged Tick*
823 *(Ixodes scapularis) (Acari: Ixodidae) in Mid-Western Pennsylvania.* J Med Entomol, 2015. **52**(6):
824 p. 1260-9.
825 30. Han, S., et al., *Seasonality of acarological risk of exposure to Borrelia miyamotoi from questing*
826 *life stages of Ixodes scapularis collected from Wisconsin and Massachusetts, USA.* Ticks Tick
827 Borne Dis, 2021. **12**(1): p. 101556.
828 31. Ogden, N.H., et al., *Evidence for Geographic Variation in Life-Cycle Processes Affecting Phenology*
829 *of the Lyme Disease Vector Ixodes scapularis (Acari: Ixodidae) in the United States.* J Med
830 Entomol, 2018. **55**(6): p. 1386-1401.
831 32. Gilmore, R.D., Jr., et al., *The bba64 gene of Borrelia burgdorferi, the Lyme disease agent, is*
832 *critical for mammalian infection via tick bite transmission.* Proc Natl Acad Sci U S A, 2010.
833 **107**(16): p. 7515-20.
834 33. Zinck, C.B., et al., *Variation among strains of Borrelia burgdorferi in host tissue abundance and*
835 *lifetime transmission determine the population strain structure in nature.* PLoS Pathog, 2023.
836 **19**(8): p. e1011572.
837 34. Dollt, C., et al., *The novel immunoglobulin super family receptor SLAMF9 identified in TAM of*
838 *murine and human melanoma influences pro-inflammatory cytokine secretion and migration.*
839 Cell Death Dis, 2018. **9**(10): p. 939.
840 35. Shachar, I., et al., *SLAMF receptors on normal and malignant B cells.* Clin Immunol, 2019. **204**: p.
841 23-30.
842 36. Kramer, A., et al., *Causal analysis approaches in Ingenuity Pathway Analysis.* Bioinformatics,
843 2014. **30**(4): p. 523-30.
844 37. Hulsen, T., J. de Vlieg, and W. Alkema, *BioVenn - a web application for the comparison and*
845 *visualization of biological lists using area-proportional Venn diagrams.* BMC Genomics, 2008. **9**:
846 p. 488.
847 38. Burgess, E.C., J.B. French, Jr., and A. Gendron-Fitzpatrick, *Systemic disease in Peromyscus*
848 *leucopus associated with Borrelia burgdorferi infection.* Am J Trop Med Hyg, 1990. **42**(3): p. 254-
849 9.
850 39. Bourgeois, B., et al., *Clobetasol increases the abundance of Borrelia burgdorferi in the skin 70*
851 *times more in male mice compared to female mice.* Ticks Tick Borne Dis, 2022. **13**(6): p. 102058.
852 40. Derdakova, M., et al., *Interaction and transmission of two Borrelia burgdorferi sensu stricto*
853 *strains in a tick-rodent maintenance system.* Appl Environ Microbiol, 2004. **70**(11): p. 6783-8.

854 41. Rynkiewicz, E.C., et al., *Closely-related Borrelia burgdorferi (sensu stricto) strains exhibit similar*
855 *fitness in single infections and asymmetric competition in multiple infections.* Parasit Vectors,
856 2017. **10**(1): p. 64.
857 42. Lindsay, L.R., et al., *Duration of Borrelia burgdorferi infectivity in white-footed mice for the tick*
858 *vector Ixodes scapularis under laboratory and field conditions in Ontario.* J Wildl Dis, 1997. **33**(4):
859 p. 766-75.
860 43. Devevey, G., et al., *First arrived takes all: inhibitory priority effects dominate competition*
861 *between co-infecting Borrelia burgdorferi strains.* BMC Microbiol, 2015. **15**: p. 61.
862 44. Johnson, R.C., et al., *Borrelia burgdorferi sp. nov.: Etiologic Agent of Lyme Disease.* International
863 Journal of Systematic and Evolutionary Microbiology, 1984. **34**(4): p. 496-497.
864 45. Marcinkiewicz, A.L., et al., *Structural evolution of an immune evasion determinant shapes*
865 *pathogen host tropism.* Proc Natl Acad Sci U S A, 2023. **120**(27): p. e2301549120.
866 46. Combs, M.A., et al., *Host adaptation drives genetic diversity in a vector-borne disease system.*
867 PNAS Nexus, 2023. **2**(8): p. pgad234.
868 47. Lemieux, J.E., et al., *Whole genome sequencing of human Borrelia burgdorferi isolates reveals*
869 *linked blocks of accessory genome elements located on plasmids and associated with human*
870 *dissemination.* PLoS Pathog, 2023. **19**(8): p. e1011243.
871 48. Earnhart, C.G., et al., *Demonstration of OspC type diversity in invasive human lyme disease*
872 *isolates and identification of previously uncharacterized epitopes that define the specificity of the*
873 *OspC murine antibody response.* Infect Immun, 2005. **73**(12): p. 7869-77.
874 49. LoGiudice, K., et al., *The ecology of infectious disease: effects of host diversity and community*
875 *composition on Lyme disease risk.* Proc Natl Acad Sci U S A, 2003. **100**(2): p. 567-71.
876 50. Sheldon, B.C. and S. Verhulst, *Ecological immunology: costly parasite defences and trade-offs in*
877 *evolutionary ecology.* Trends Ecol Evol, 1996. **11**(8): p. 317-21.
878 51. Sadd, B.M. and P. Schmid-Hempel, *Principles of ecological immunology.* Evol Appl, 2009. **2**(1): p.
879 113-21.
880 52. Barthold, S.W., et al., *Lyme borreliosis in selected strains and ages of laboratory mice.* J Infect
881 Dis, 1990. **162**(1): p. 133-8.
882 53. Yang, L., et al., *Heritable susceptibility to severe Borrelia burgdorferi-induced arthritis is*
883 *dominant and is associated with persistence of large numbers of spirochetes in tissues.* Infect
884 Immun, 1994. **62**(2): p. 492-500.
885 54. Steppan, S., R. Adkins, and J. Anderson, *Phylogeny and divergence-date estimates of rapid*
886 *radiations in muroid rodents based on multiple nuclear genes.* Syst Biol, 2004. **53**(4): p. 533-53.
887 55. Johnson, R.C., N. Marek, and C. Kodner, *Infection of Syrian hamsters with Lyme disease*
888 *spirochetes.* J Clin Microbiol, 1984. **20**(6): p. 1099-101.
889 56. Rathinavelu, S., A. Broadwater, and A.M. de Silva, *Does host complement kill Borrelia burgdorferi*
890 *within ticks?* Infect Immun, 2003. **71**(2): p. 822-9.
891 57. de Silva, A.M., et al., *OspA antibodies inhibit the acquisition of Borrelia burgdorferi by Ixodes*
892 *ticks.* Infect Immun, 1997. **65**(8): p. 3146-50.
893 58. Helble, J.D., et al., *Single-cell RNA sequencing of murine ankle joints over time reveals distinct*
894 *transcriptional changes following Borrelia burgdorferi infection.* iScience, 2023. **26**(11): p.
895 108217.
896 59. Barbour, A.G., *Isolation and cultivation of Lyme disease spirochetes.* Yale J Biol Med, 1984. **57**(4):
897 p. 521-5.
898 60. Kent, W.J., et al., *The human genome browser at UCSC.* Genome Res, 2002. **12**(6): p. 996-1006.
899 61. Dobin, A., et al., *STAR: ultrafast universal RNA-seq aligner.* Bioinformatics, 2013. **29**(1): p. 15-21.
900 62. Li, B. and C.N. Dewey, *RSEM: accurate transcript quantification from RNA-Seq data with or*
901 *without a reference genome.* BMC Bioinformatics, 2011. **12**: p. 323.

902 63. Love, M.I., W. Huber, and S. Anders, *Moderated estimation of fold change and dispersion for*
903 *RNA-seq data with DESeq2.* Genome Biol, 2014. **15**(12): p. 550.

904